Bioorganic Chemistry 171 (2026) 109567

Contents lists available at ScienceDirect

Bioorganic Chemistry

journal homepage: www.elsevier.com/locate/bioorg

Adenine nucleotides as potent and selective GPR17 modulators

Diego Dal Ben *, Catia Lambertucci, Michela Buccioni, Beatrice Francucci, Andrea Spinaci, Rosaria Volpini, Gabriella Marucci

School of Pharmacy, Medicinal Chemistry Unit, University of Camerino, Via Madonna delle Carceri, I-62032 Camerino, Italy

ARTICLE INFO

Keywords:
GPR17
cAMP assay
Nucleotides
ATP derivatives
GloSensor
Luciferine–luciferase system
Leukotrienes
Oligodendrocytes

ABSTRACT

The G protein-coupled receptor GPR17 is expressed by neuronal cells in various brain areas, where it modulates oligodendrocytes maturation and differentiation and myelination process. The altered expression and activity of this receptor are associated with neurodegenerative processes like myelinating disorders, brain ischemia, and multiple sclerosis. Hence, the development of pharmacological tools able to modulate GPR17 activity may represent a potential key strategy to treat CNS disorders. In this work, we developed adenine nucleotides consisting in 5′-triphosphate derivatives, their α,β- or β,γ-modified triphosphate analogues, and 3′,5′-bisphosphate derivatives, with the adenine core presenting further modifications given by the presence of substituents at the 2- and/or N^6-position. Results of biological evaluation at HEK293 L9–2 cells transiently transfected with human GPR17 demonstrated that the novel compounds are endowed with nanomolar or picomolar potency and various profiles of efficacy. GPR17 selectivity of these molecules was also demonstrated by evaluating them at HEK293 L9–2 cells transiently transfected with human purinergic $P2Y_{12}$, $P2Y_{13}$, and $P2Y_{14}$ receptors.

1. Introduction

The screening of G protein-coupled receptors (GPCRs) has long been an attractive strategy for pharmacological intervention due to their involvement in many major diseases. Among these integral membrane proteins, GPR17 was identified as a GPCR implicated in neurodegenerative processes. In physiological conditions, GPR17 is expressed by neuronal cells belonging to various brain areas including a subset of adult quiescent parenchymal oligodendrocyte progenitors [1]. After ischemia, GPR17 is further induced in microglia and adult oligodendrocyte precursor cells, suggesting its regulatory role in response mechanisms to injury in embryonically distinct cell types. In fact, a key role of this system was hypothesized in the progression of brain ischemic damage [1–4].

The expression of GPR17 on oligodendrocytes has also been linked to the myelination process. GPR17 was found to be downregulated in oligodendritic cells during the peak period of myelination and in adulthood. Furthermore, myelinating disorders were observed in transgenic mice with enhanced GPR17 expression, while GPR17 knockout mice displayed early onset of oligodendrocyte myelination [5]. Contrary to this, data from Abbracchio and co-workers clearly argue for a role of GPR17 in driving and promoting oligodendrocyte maturation and differentiation, as demonstrated by the enhanced number of oligodendrocyte precursor cells and of cells expressing anti-myelin basic protein after exposure to GPR17 agonists like UDP-glucose [6–8]. Despite these varying results, GPR17 represents a possible target for drug discovery in neurodegenerative diseases, including cerebral ischemia [2], traumatic brain injury [9], spinal cord injury [10], and demyelinating diseases such as multiple sclerosis [6,11].

Two isoforms of human GPR17 have been revealed in the brain [12,13]. A short isoform, presenting 339 amino acids and showing a strong expression in the brain, was the first GPR17 isoform that revealed dual responses to uracil nucleotides and cysteinyl leukotrienes (CysLTs). The long GPR17 isoform, a protein of 367 amino acids, is a functional receptor with an exclusive presence in brain, suggesting highly specific roles in the nervous system [14,15].

Several studies demonstrated that GPR17 stimulation leads to decrease of intracellular cAMP formation through stimulation of $G\alpha_{i/o}$ protein and consequent decrease of adenylyl cyclase activity. Further results suggested also that under some circumstances the GPR17 stimulation can modulate intracellular calcium levels [6,16,17]. As mentioned, GPR17 initially showed a peculiar dual pharmacology by

Abbreviations: GPCR, G protein-coupled receptor;; CysLTs, Cysteinyl leukotrienes;; FAC-MS, Frontal affinity chromatography combined with mass spectroscopy;; ATP, Adenosine-5'-*O*-triphosphate;; TLC, Thin-layer chromatography;; ESI-MS, Electrospray ionization mass spectrometry;; FBS, Fetal bovine serum.

* Corresponding author.
E-mail address: diego.dalben@unicam.it (D. Dal Ben).

https://doi.org/10.1016/j.bioorg.2026.109567
Received 3 November 2025; Received in revised form 21 January 2026; Accepted 26 January 2026
Available online 27 January 2026

being activated by uracil nucleotides (UDP, UDP-glucose, and UDP-galactose) and CysLTs (CysLT C4 and CysLT D4) [1]. This is in accordance with the phylogenetic characterization of the receptor, which has been positioned as intermediate between purinergic P2Y and CysLT receptors, even if recent works suggest a potential phylogenetic correlation with additional receptors [1,18]. Furthermore, inhibitors of the P2Y and CysLT receptors modulated GPR17 signaling, confirming this dualism in which the orthosteric site is where nucleotides bind, whereas CysLTs are allosteric ligands. Subsequently, Benne-Jensen et al. confirmed the GPR17 ligand-binding profile for uracil nucleotides in transiently transfected HEK293 cells [15]. Further screening of various synthetic adenine and uracil nucleotides on the GPR17 receptor using either a [^{35}S]GTPγS binding assay or a frontal affinity chromatography combined with mass spectroscopy (FAC-MS) confirmed the nucleotide binding site [19]. It must be noted that the GPR17 modulation by native or synthetic nucleotides has been contradicted by other research groups. Maekawa et al. obtained no response to UDP-glucose in 1321N1 cell clones stably expressing mouse GPR17 [20]. Total lack of activation by UDP and its sugar conjugates was outlined by Qi *et al* at GPR17 stably expressed in C6, 1321N1, and CHO cells or transiently expressed in COS-7 and HEK293 cells [21]. Likewise, also the binding of Cys-LTs to transfected GPR17 still lacks consensus. Heise et al. observed no calcium-dependent chloride conductance in response to LTC_4 or LTD_4 in GPR17 cRNA-injected *Xenopus laevis* oocytes [22]. Benned-Jensen et al. in HEK293 cells, Maekawa et al. in 1321N1, CHO or HEK-293 T cells, and Qi et al. in C6, 1321N1, CHO, COS-7 or HEK293 cells obtained no biological recognition to Cys-LTs [15,20,21]. In addition, GPR17 ligands have been identified bearing different structural characteristics from nucleotides and CysLTs. A class of indolic derivatives was then patented as GPR17 modulators, of which the compound MDL29,951 (Fig. 1) was reported as agonist and used for further receptor characterization [11,16,23,24]. More recent studies described the identification or development of GPR17 modulators based on various structural classes, whose activity was interpreted based on an orthosteric or allosteric mechanism of action [25–29].

The experimental 3D structure of the human GPR17-G_i complex was also recently reported, obtained with cryo-EM technique [30]. This structure was obtained in the ligand-free state and suggests a self-activation mechanism induced by the extracellular loop 2 (EL2) domain of the protein, potentially associated with a high level of basal signaling. The structure also suggests the presence of a hydrophilic orthosteric binding pocket. This clearly creates a need for through pharmacological characterization of the GPR17 receptor, identification of its endogenous ligand(s), and development of potent and selective synthetic modulators with therapeutic potential [31].

Our research group furnished the first set of ligands for the GPR17 receptor [19,32], with 2-phenylethynyladenosine-5'-*O*-triphosphate (**1**, Fig. 1) showing a remarkable agonist profile. This adenosine-5'-*O*-triphosphate (ATP) analogue, bearing a large and lipophilic substituent in the 2-position, displayed EC_{50} values of 35 pM in GloSensor cAMP assay and 36 pM in [^{35}S]GTPγS binding assay [32]. This data was also confirmed by a longer retention time of **1** in FAC-MS screening methodology performed on GPR17 entrapped on immobilized artificial membrane [19].

Starting from these observations and with the aim of finding new potent GPR17 ligands, new adenine nucleotides were designed and synthesized. Firstly, we probed the N^6-position of **1** by designing and synthesizing an ATP derivative bearing a phenylethynyl chain in the 2-position combined with a N^6-methyl substitution (Fig. 2).

Taking into account the low chemical stability of the triphosphate chain particularly in biological mediums, and based on other key ATP stable analogues like *i.e.* α,β-methyleneATP (reference P2 receptor ligand), a new analogue of **1** endowed with higher stability was designed and synthesized by substituting its 5'-*O*-triphosphate group with a 5'-*O*-α,β-methylenetriphosphate function (Fig. 2). Furthermore, Cangrelor (Fig. 1), a nucleotide derivative bearing a β,γ-dichloromethylene spacer within its triphosphate chain showed to behave as a nucleotidic GPR17 antagonist endowed with IC_{50} value of 0.7 nM in [^{35}S]GTPγS binding assay [19]. Based on this data, and taking into account the previously reported observations that the substitution of the β,γ-oxygen atom of 2-MeS-ATP with a dichloromethylene spacer enhanced the stability of the compound in human blood serum samples and when exposed to ecto-5′-nucleotidases activity [33], we analogously substituted the 5'-*O*-triphosphate group of **1** with a 5'-*O*-β,γ-dichloromethylenetriphosphate chain (Fig. 2).

On the other hand, MRS 2179 and **2** (Fig. 1), two previously reported GPR17 antagonists, are endowed with IC_{50} values of 508 nM and 582 nM, respectively [19]. Considering that these two GPR17 antagonists are structurally 2′-deoxy-3′,5′-bisphosphate nucleotide derivatives, a corresponding analogue of **1** bearing the 2-phenylethynylic group was

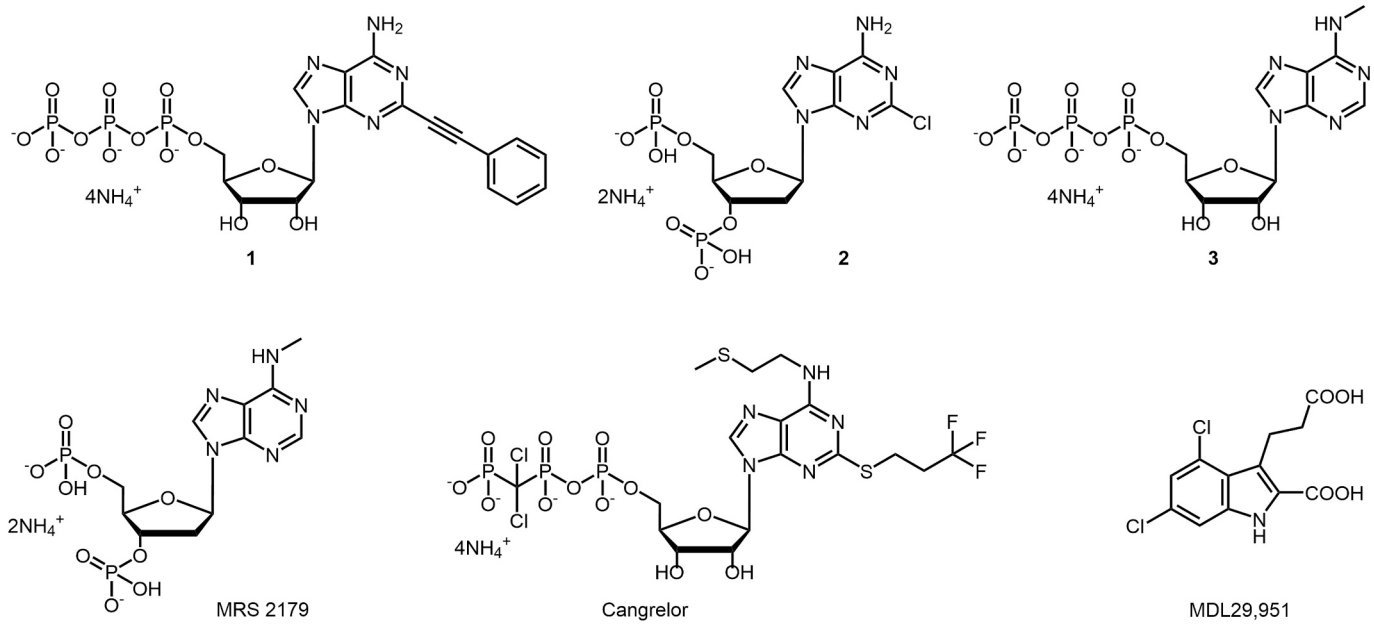

Fig. 1. Structures of some known GPR17 ligands.

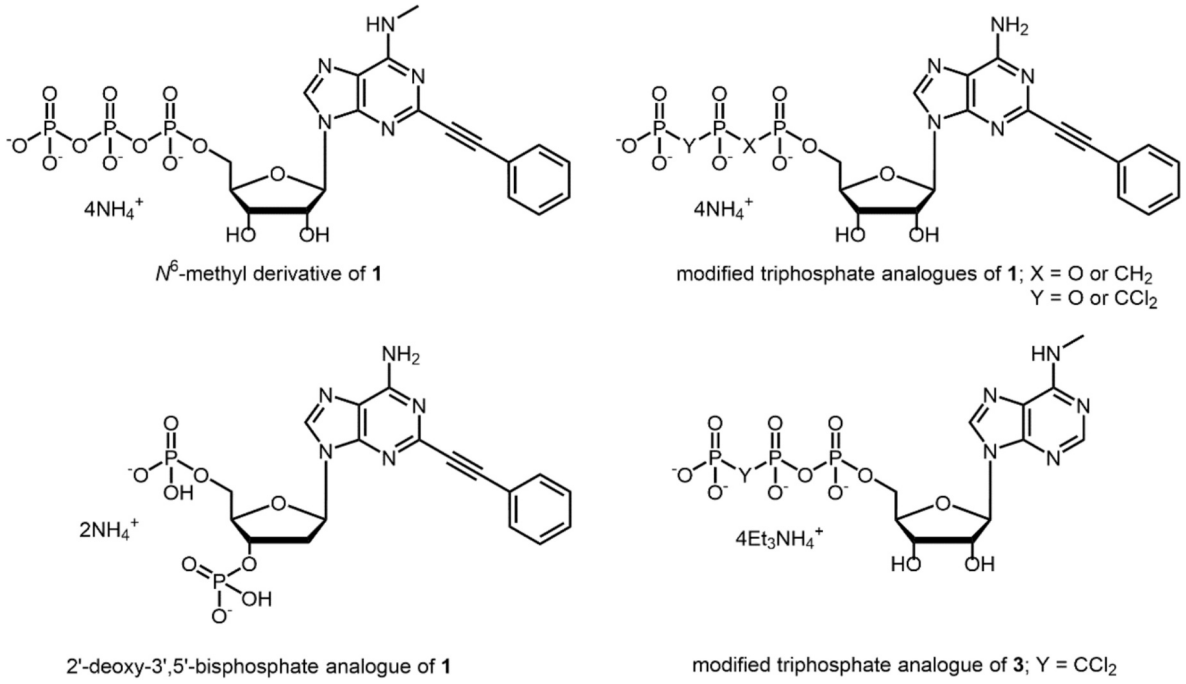

Fig. 2. Structures of newly synthesized GPR17 ligands.

synthesized (Fig. 2). Among the same set of triphosphates previously synthesized [19], N^6-methylATP (**3**, Fig. 1) showed a nanomolar activity at the GPR17 receptor, precisely IC_{50} values of 144 nM in GloSensor cAMP assay and 112 nM in [^{35}S]GTPγS binding assay [32]. Analogously to Cangrelor, **3** was modified by substituting the 5'-*O*-triphosphate group with a 5'-*O*-β,γ-dichloromethylenetriphosphate chain (Fig. 2).

All newly synthesized derivatives were tested at HEK293 L9–2 cells transiently transfected with hGPR17 by using the sensitive and non-radioactive GloSensor cAMP assay. This experiment evaluates a GPCR activity by monitoring the variation of the intracellular cAMP concentration with the aid of a mutant form of *Photinus pyralis* luciferase [32]. Since triphosphate or bisphosphate adenine derivatives could be endowed with activity at the purinergic P2Y receptors, we evaluated the selectivity of the newly synthesized compounds by testing them also at HEK293 L9–2 cells transiently transfected with $hP2Y_{12}$, $hP2Y_{13}$, and $hP2Y_{14}$ by using the same assay. These receptors were selected given their functional coupling with a $G\alpha_{i/o}$ protein, whose activation leads to inhibition of adenylyl cyclase and decrease of intracellular cAMP (analogously to GPR17).

2. Results and discussion

2.1. Chemistry

The nucleotides and nucleotide analogues **8**–**10**, **13**, and **16** were prepared following various procedures as portrayed in Schemes 1–4. The synthesis of triphosphates **8–10** (Schemes 1 and 2) was undertaken *via* the protected 6-chloro-2-iodopurineriboside **4**, obtained from commercially available guanosine in three steps [34]. Reaction of **4** with phenylethyne gave the 2-phenylacetylene analogue **5** *via* a palladium/copper-catalyzed Sonogashira reaction. Reaction of the latter compound, in turn, with the appropriate amines permitted 6-amination and the deprotection of the sugar moiety providing the desired 2,6-disubstituted adenosine derivatives **6** and **7** (Scheme 1).

These nucleosides were phosphorylated using different synthetic approaches based on the type of triphosphate intended as shown in Scheme 2. Nucleoside **7** was treated with phosphorus oxychloride and then with tributylammonium pyrophosphate in basic conditions by using proton sponge to afford the triphosphate nucleotide **8**.

The $P_\alpha P_\beta$-methylene analogue of **1** was obtained by reacting nucleoside **6** initially with methylenebis(phosphonic dichloride) and then with tributylammonium monophosphate in presence of proton sponge furnishing the desired 2-phenylethynyl-α,β-methyleneATP (**9**). To prepare 2-phenylethynyl-β,γ-dichloromethyleneATP (**10**), 2-phenylethynyladenosine (**6**) was subjected to phosphorylation using phosphorus oxychloride followed by reaction with bis-(tri-*n*-butylammonium) dichloromethylenediphosphonate in DMF and final quenching by addition of a cold 0.5 M aqueous TEAB solution [35].

The bisphosphate derivative **13** (Scheme 3) was synthesized starting from 2-iodo-2′-deoxyadenosine (**11**), which was obtained as reported in literature [36]. Hence, **11** was reacted with phenylacetylene, using the Sonogashira cross coupling reaction, to obtain the 2-phenylethynyl-2′-

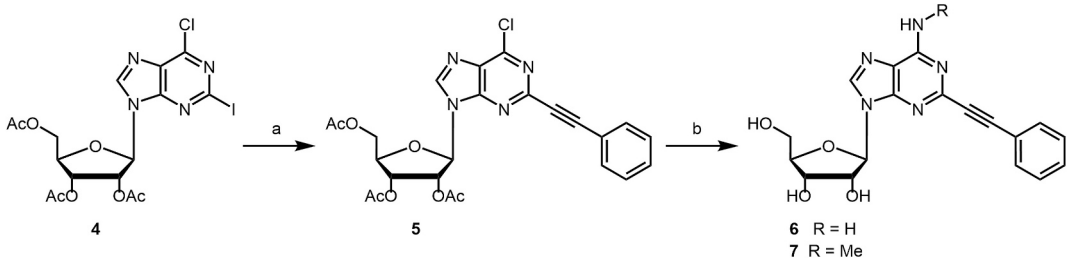

Scheme 1. Reagents and conditions: a. phenylacetylene, $(PPh_3)_2PdCl_2$, CuI, TEA, DMF, r.t., 3 h; b. NH_3, r.t., 16 h or CH_3NH_2, r.t., 30 min.

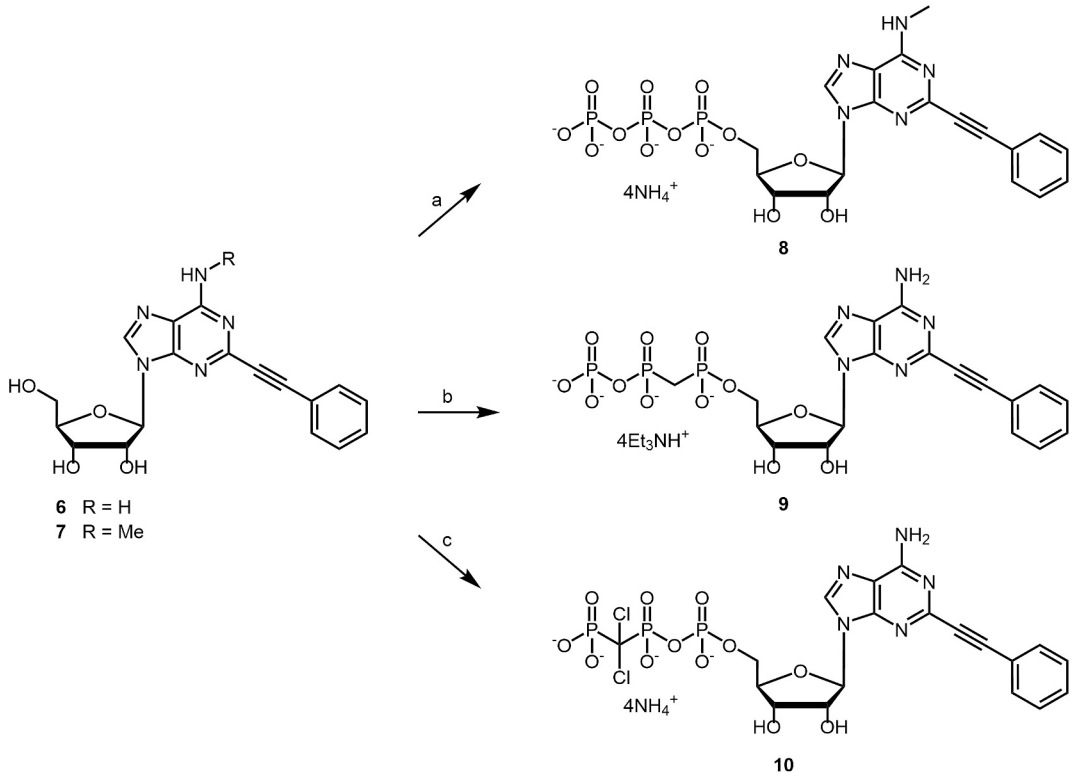

Scheme 2. Reagents and conditions: a. (i) $POCl_3$, proton sponge, $PO(OCH_3)_3$, (ii) $(n Bu_3N)_2H_4P_2O_7$, $n Bu_3N$, Et_3NHHCO_3, 0 °C to r.t., 5 h; b. (i) $CH_2(PO)_2Cl_4$, proton sponge, $PO(OCH_3)_3$, (ii) $(n Bu_3N)H_3PO_4$, $n Bu_3N$, 0 °C to r.t., 7 h; c. (i) $POCl_3$, proton sponge, $PO(OCH_3)_3$, (ii) $CH_2Cl_2Na_2O_6P_2$, $n Bu_3N$, DMF, 0 °C to r.t., 6 h.

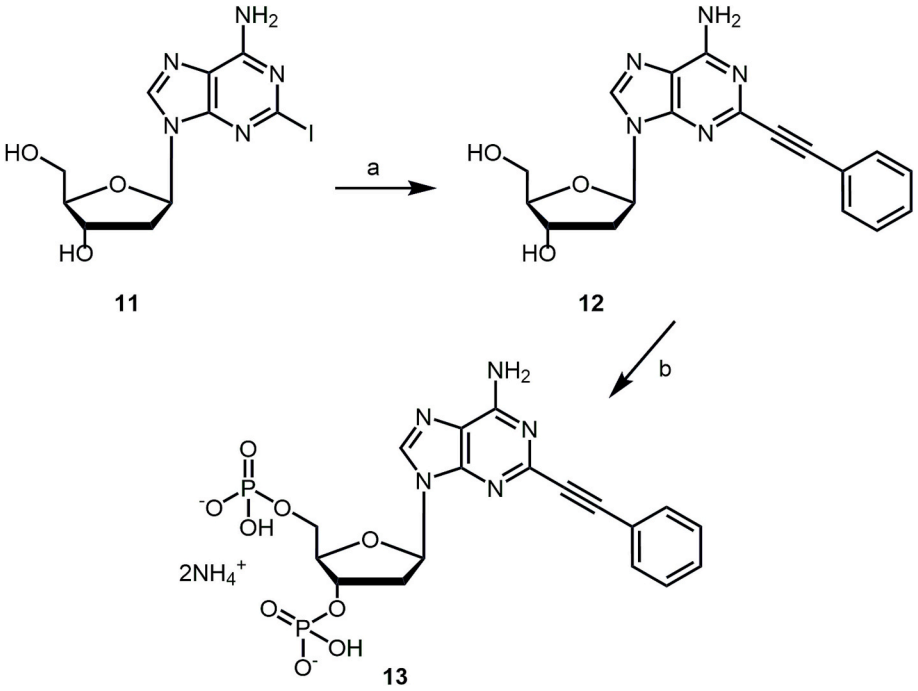

Scheme 3. Reagents and conditions: a. phenylacetylene, $(PPh_3)_2PdCl_2$, CuI, TEA, DMF, r.t., 7 h; b. $POCl_3$, proton sponge, $PO(OCH_3)_3$, 0 °C to r.t., 1 h.

deoxyadenosine (**12**), which was treated with phosphorus oxychloride in the presence of proton sponge and trimethylphosphate as solvent to give the desired bisphosphate analogue **13**.

The N^6-methylATP analogue bearing 5'-*O*-β,γ-dichloromethylenetriphosphate (**16**) was obtained from commercial adenosine in a three-step synthetic procedure (Scheme 4). A typical Sandmeyer reaction on adenosine granted the 6-iodo-9-(*β*-D-ribofuranosyl)purine (**14**), which upon reaction with methylamine afforded N^6-methyladenosine (**15**). The phosphorylation of **15** was performed using the same procedure for the preparation of **10**.

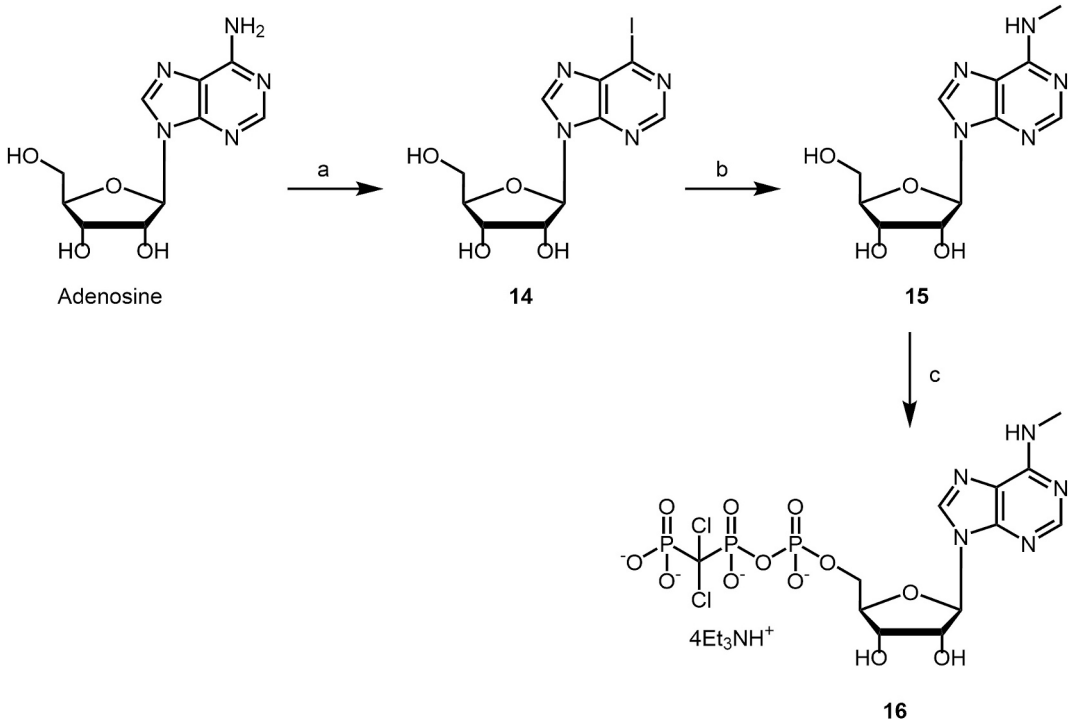

Scheme 4. Reagents and conditions: a. CH_2I_2, isoamyl nitrite, DMF, 60 °C, 30 min; b) CH_3NH_2, r.t., 3 h; c) (i) $POCl_3$, proton sponge, $PO(OCH_3)_3$, (ii) $CH_2Cl_2Na_2O_6P_2$, nBu$_3$N, DMF, 0 °C to r.t., 6 h.

2.2. Biological evaluation

All the synthesized compounds, **8**–**10**, **13**, and **16** (and also the already reported compound **2**), were tested by using the non-radioactive GloSensor cAMP assay on HEK293 L9–2 cells transiently transfected with hGPR17 [32]. This GloSensor cAMP assay involves a non-lytic protocol, which permits the evaluation of GPCR activity in live cells. This assay uses a biosensor technology in which a cAMP binding domain is inserted into *Photinus pyralis* luciferase. The binding of cAMP induces conformational changes that promote large increases in light output allowing the evaluation of ligand activity at the receptor under study [37,38].

All the tested compounds were able to activate or antagonize to various extent the studied receptor, behaving as GPR17 receptor agonists or antagonists. Fig. 3 shows dose-response curves of agonists **8**–**10**, and **13** and antagonists **2** and **16**. Furthermore, these compounds gave no response in cells transfected with the empty vector, demonstrating a specific effect on the GPR17 receptor.

The triphosphate-modified analogues of **1** maintained high activity at the hGPR17, as shown in Table 1. Compound **9**, bearing the 5'-*O*-α,β-methylenetriphosphate, displayed an activity 16-fold lower than the parent triphosphate **1** (**1**, EC_{50} = 35 pM *vs* **9**, EC_{50} = 0.57 nM). The 5'-*O*-β,γ-dichloromethylenetriphosphate analogue **10** instead, maintained an EC_{50} of 62 pM, a very similar profile compared to **1** (EC_{50} = 35 pM).

On the other hand, the modification of the GPR17 antagonist N^6-methylATP (**3**) by substituting its triphosphate chain with a β,γ-dichloromethylenetriphosphate group, led to compound **16** presenting a 11-fold increase of activity (**16**, IC_{50} = 13 nM *vs* **3**, IC_{50} = 144 nM) at the GloSensor cAMP assay. The substitution of the 2-chlorine atom on previously reported 2′-deoxy-3′,5′-bisphosphate **2** with a

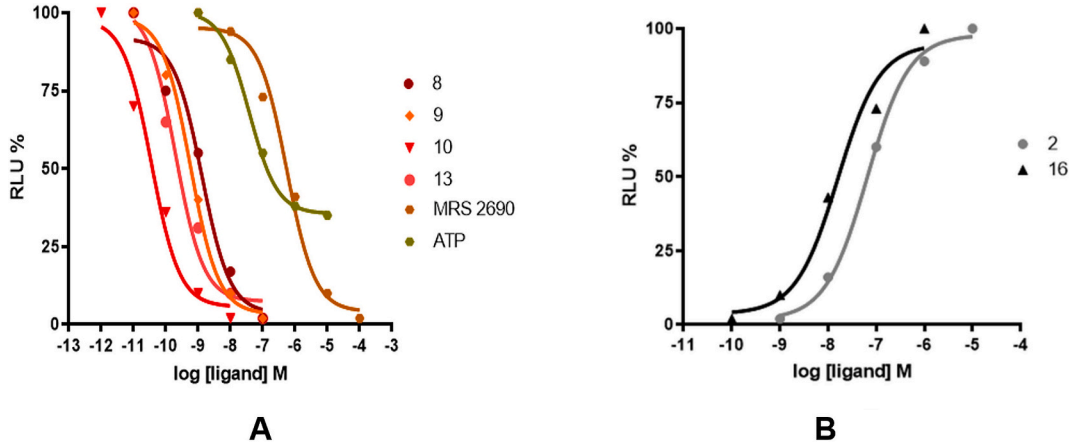

Fig. 3. Dose–response curves on HEK293 L9–2 cells transiently transfected with hGPR17 of agonists **8**–**10**, and **13**, in comparison with **MRS 2690** and **ATP** [32] used as reference agonists (**A**), and antagonists **2** and **16** (**B**). Forskolin (10 μM) was used to increase basal level of cAMP. Data are expressed as mean of three-four experiments performed in duplicate, with a maximum SE lower than ±10.

Table 1
Biological activity and response of the compounds evaluated by using the GloSensor cAMP assay at HEK293 L9–2 cells transiently transfected with hGPR17.

Cpd	R	R_1	X	Y	Response %[a]	EC_{50} (nM)[b]	IC_{50} (nM)[c]
Triphosphate and triphosphate-modified derivatives							
1	-C≡C-Ph	H	O	O	100 ± 0.04	35 ± 3 pM [32]	–
9	-C≡C-Ph	H	CH_2	O	100 ± 0.02	0.57 ± 0.03	–
10	-C≡C-Ph	H	O	CCl_2	100 ± 0.03	62 ± 4 pM	–
8	-C≡C-Ph	CH_3	O	O	100 ± 0.03	1.6 ± 0.1	–
3	H	CH_3	O	O	–	–	144 ± 18 [32]
16	H	CH_3	O	CCl_2	–	–	13 ± 1
2′-deoxy-3′,5′-bisphosphate derivatives							
2	Cl	–	–	–	–	–	69 ± 10
13	-C≡C-Ph	–	–	–	100 ± 0.01	0.15 ± 0.02	–

[a] Response is expressed as percentage of the maximal relative luminescence units and is referenced against UDP (used as a reference compound at the concentration of 100 nM), set at 100%.
[b] Compound concentration needed to produce 50% of the maximum effect, expressed as EC_{50} nM unless noted.
[c] Compound concentration needed to produce 50% inhibition of agonist effect. Each concentration was tested five times in triplicate, and values are given as the mean ± SE.

phenylethynyl group led to compound **13**. Results from the cAMP-based assay highlighted a complete change of activity. Differently from **2**, an antagonist showing IC_{50} value of 69 nM at the hGPR17, the presence of the phenylethynyl moiety at the 2-position of **13** afforded a potent agonist with EC_{50} of 0.15 nM. These results confirm the high agonistic activity of compounds bearing the 2-phenylethynyl moiety at the hGPR17 (as confirmed also by the fact that α,β-methyleneATP was inactive at the hGPR17 compared to its 2-modified analogue, **9**) and raises interrogations on the mode of interaction between this substituent and the receptor protein. The insertion of a N^6-methyl substituent on **1** led to a 45-fold decrease of compound potency (**1**, EC_{50} = 35 pM *vs* **8**, EC_{50} = 1.6 nM), indicating that an unsubstituted 6-amine group provides a better interaction with the receptor binding site compared to a N^6-substituted triphosphate analogue.

Given that triphosphate or bisphosphate adenine derivatives could be endowed with activity at the purinergic P2Y receptors, we evaluated the activity of the three compounds **1**, **9**, and **10** (showing GPR17 agonist profile) at the three P2Y receptor subtypes $hP2Y_{12}$, $hP2Y_{13}$, and $P2Y_{14}$, which are coupled to $G\alpha_{i/o}$ protein like GPR17. The results are reported in Table 2. The aim of this task was to evaluate the selectivity of the above cited three molecules (at concentrations analogue to their EC_{50} values) *versus* these three P2Y receptor subtypes that functionally couple with the same second messenger of GPR17, to analyze if the observed decrease of cAMP could be due also to a P2Y modulation. For this test, three preparations of HEK293 L9–2 cells were transiently transfected with $hP2Y_{12}$, $hP2Y_{13}$, and $hP2Y_{14}$, respectively. The activity at these receptors was measured again by using the non-radioactive GloSensor cAMP assay. P2Y modulators like ADP, UDP-glucose, MRS 2690 [39], and the non-nucleotidic GPR17 agonist MDL29,951 [11,16,23] were also tested.

Table 2
Biological activity (EC_{50}, nM unless noted) of the selected compounds **1**, **9**, and **10** at HEK293 L9–2 cells transiently transfected with $hP2Y_{12}$, $hP2Y_{13}$, and $hP2Y_{14}$, using the GloSensor cAMP assay. The activity at the hGPR17 is shown for comparison.

Compound	GPR17	$P2Y_{12}$	$P2Y_{13}$	$P2Y_{14}$
UDP-glucose	12,565 ± 2,760	> 30,000	> 30,000	660 ± 112
ADP	82 (55%) ± 14	223 ± 34	13 ± 1.74	> 30,000
1	35 ± 3 pM	1,348 ± 194	3,388 ± 498	178 ± 27
9	0.57 ± 0.03	19,952 ± 2,854	7,413 ± 1,036	776 ± 127
10	62 ± 4 pM	7,585 ± 984	4,455 ± 640	141 ± 24
MRS 2690	553 ± 98	17,378 ± 2,416	> 30,000	70 ± 11
MDL29,951	108 ± 18	> 30,000	> 30,000	> 30,000

MDL29,951 did not modulate the P2Y receptors and showed a high nanomolar potency as GPR17 agonist, in agreement with previously reported results [11]. MRS 2690 showed nanomolar potency at the $P2Y_{14}$, analogously to what previously published [39]. Evaluation of **1**, **9**, and **10** showed that these molecules are active at the three P2Y receptor subtypes considered for this study, even if at concentrations ranging from high-nanomolar to micromolar levels. Hence, the potencies of these compounds measured at the GPR17 are thousand-fold higher than the ones at the $hP2Y_{12}$, $hP2Y_{13}$, and $hP2Y_{14}$. These results demonstrate that at the picomolar concentrations needed to obtain a decrease of cAMP through GPR17 stimulation, **1**, **9**, and **10** have a substantially null effect at the analyzed P2Y receptors, proving the selectivity of these molecules for the GPR17 receptor.

2.3. Molecular modeling

The potential binding mode of the synthesized compounds at the hGPR17 was simulated with the aid of molecular modeling tools. Since the available cryo-EM structure of the hGPR17 (pdb code: 7Y89 [30]) was obtained in an apo form, we developed a homology model of the same protein by using the crystal structure of the human $P2Y_{12}$ receptor in complex with the agonist 2-methylthio-ADP (pdb code: 4PXZ [40]) as a template. The hGPR17 experimental structure and homology model present the same general architecture, with the main difference consisting in the arrangement of the EL2 domain, whose conformation in the homology model leaves open the access to the hypothetical transmembrane binding site. The homology modeling study, together with receptor model refinement with energy minimization tools, was performed within Molecular Operating Environment (MOE2022.02) Suite [41]. Docking experiments of the synthesized compounds were performed by using the Induced Fit docking protocol of MOE and the genetic algorithm docking tool of CCDC Gold [42]. The most frequent top-score conformations for each compound were selected for the analysis of the ligand-target interaction.

The results of the docking studies provide a suggestion of a potential binding mode of the compounds at the receptor. In detail, for the triphosphate and triphosphate-modified analogues (Fig. 4), docking results suggest a conformation in which the triphosphate and triphosphate-modified chain gets inserted between residues Tyr66 (TM1), Arg115 (TM2), His119 (TM2), Gln211 (EL2), Tyr279 (TM6), Arg283 (TM6), Asn307 (TM7), Arg308 (TM7), and Ser311 (TM7). The ribose group makes a polar interaction with the alpha-phosphate group and interacts with residues Tyr286 (TM6) and Asn307 (TM7). The adenine moiety makes non-polar interaction with Gly52 (N-term), Val208 (EL2), and Leu210 (EL2). Potential additional interaction is given with Tyr118 (TM2) and Ala304 (TM7).

The 2-substituent points toward residues of TM6 and TM7 domains. In the case of the agonists, their 2-phenylethynyl chain gets inserted in a small aromatic cluster of residues like Tyr286 (TM6), His289 (TM6), and Tyr290 (TM6). Additional non-polar interaction may occur with Leu303 (TM7) and Ala304 (TM7). The agonist activity of the compounds bearing a 2-phenylethynyl chain could be related to the stacking interaction of this substituent and the protein domains TM6–7, which is not possible for compounds unsubstituted at the 2-position and endowed with partial agonist (*i.e.* ATP [32]) or antagonist activity.

The N^6 amine group makes polar interaction with Glu54 (N-term) carboxyl function. The presence of an additional methyl group appears

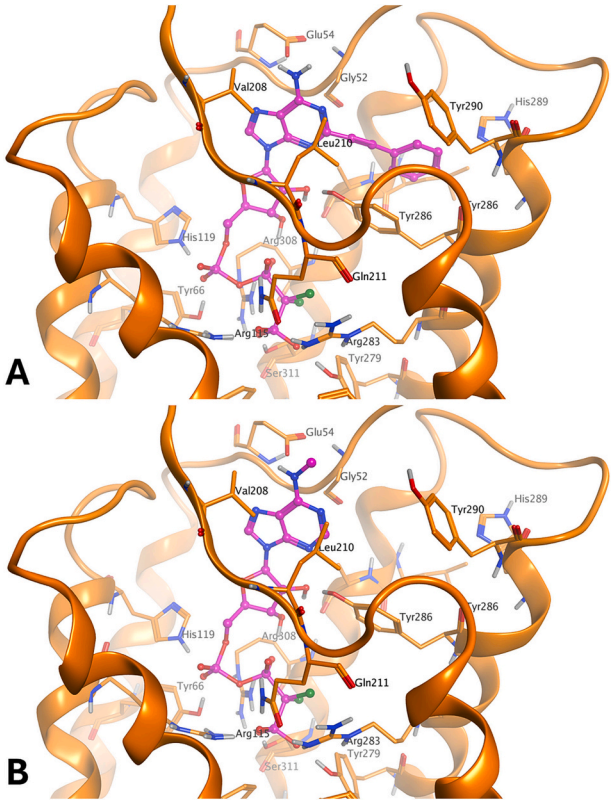

Fig. 4. Docking results for the triphosphate and triphosphate-modified derivatives. Docking conformation of agonist **10** (A) and antagonist **16** (B) are shown. Key residues for interaction with ligands are indicated.

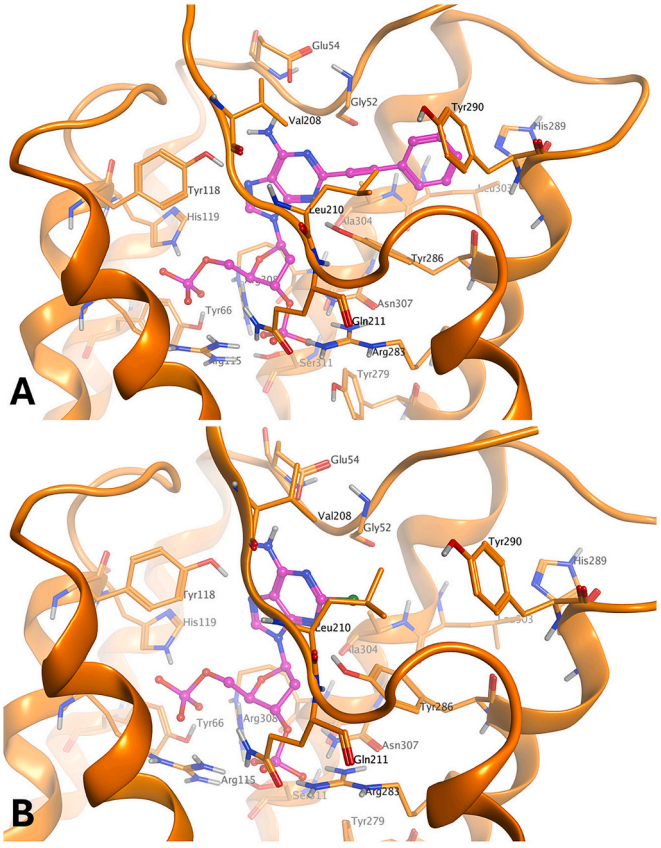

Fig. 5. Docking results for the bisphosphate derivatives. Docking conformation of agonist **13** (A) and antagonist **2** (B) are shown. Key residues for interaction with ligands are indicated.

to disrupt this interaction, and this could explain the lower activity of the compounds bearing an N^6 aminomethyl group compared to the corresponding analogues bearing an N^6 unsubstituted amine (compare *i.e.* **1**: EC_{50} = 35 pM with **8**: EC_{50} = 1.6 nM). The presence of this substituent was reported also to switch the partial agonist activity of ATP to antagonist [32]).

In the case of the bisphosphate analogues (Fig. 5), docking results suggest a conformation providing a similar orientation and interaction of the adenine moiety compared to the triphosphate and triphosphate-modified analogues. Analogously, the 2-substituent points toward TM6 and TM7 residues. The bisphosphate chain makes similar interaction with the protein compared to the triphosphate and triphosphate-modified analogues as well. In detail, the 5-phosphate group makes polar interaction with residues Tyr66 (TM1), Arg115 (TM2), and His119 (TM2), while the 3-phosphate group interacts with Arg115 (TM2), Gln211 (EL2), Arg283 (TM6), Asn307 (TM7), Arg308 (TM7), and Ser311 (TM7).

Taken together these observations, docking results suggest a strong polar interaction between the phosphate groups and charged or polar non-charged protein residues in particular of TM2, TM6, and TM7. The 2-substituent appears critical to provide an additional interaction between the compounds and TM6-TM7 residues that could explain the agonist activity of the derivatives bearing a 2-phenylethynyl group. Furthermore, also the presence of the methyl group at the N^6-position seems to be important in defining the activity of the compounds by lowering the very high potency of agonist (compare with **1** with **8**) or shifting the partial agonist activity to antagonist (compare the partial agonist ATP with **3**). In any case, the limited number of compounds does not allow a well defined structure-activity relationship analysis, which could be more reliable with the development of further compounds in this series. An exploration of various substituents in the 2- and N^6-position, and their combinations, could be of help to better interpret their roles in the biological activity of the compounds.

This work aligns with other previously published works that proposed the position of the binding site of this receptor, providing interpretation of compounds activity based on ligand-target interaction suggested by docking experiments. On the other hand, to date, the position and properties of the GPR17 binding site are still to be definitively identified and the binding mode described in this work for the developed compounds is to be considered as hypothetical.

2.4. Pharmacokinetic parameters prediction

Given the key role of GPR17 in the central nervous system, the prediction of pharmacokinetic parameters of compounds targeting this receptor could be of help to evaluate the ability of these molecules to penetrate the brain. In this sense, for the newly synthesized compounds **8**–**10**, **13**, and **16** and the already reported **1**–**3** derivatives we performed an *in silico* prediction by using Molecular Operating Environment (MOE) suite software and tools downloaded from the SVL Exchange web portal (https://svl.chemcomp.com/) and then used through MOE suite interface. In detail, we predicted parameters like logP, TPSA, H-bond donors and acceptors, and specific score parameters for brain penetration like the CNS BBB Score [43] and the CNS MPO [44] descriptor. These two parameters combine various descriptors to obtain scores indicating if a compound has high or low probability to penetrate the blood–brain barrier. These parameters were calculated at the DeepPK web page (https://biosig.lab.uq.edu.au/deeppk/) and inserted in Table 3.

An *in silico* prediction of the triphosphate and triphosphate-modified chains stability was not performed. Furthermore, as expected, all the compounds are predicted to have low-to-null brain penetration. As consequence, a potential administration of these compounds for *in vivo*

Table 3
Prediction of pharmacokinetic parameters.

Compound	logP	TPSA Å^2	H-bond acc	H-bond don	CNS_BBB[a]	CNS-MPO[b]
1	−2.38	269.65	16	4	1.52	3.00
9	−2.81	260.42	15	4	1.53	2.90
10	−0.93	257.26	15	3	1.94	3.00
8	−2.06	255.66	16	4	1.47	3.00
3	−4.80	255.66	16	4	2.14	3.00
16	−3.35	243.27	15	3	1.57	2.17
2	−2.22	206.05	12	3	2.36	3.14
13	−0.44	206.05	12	3	1.76	2.74

[a] CNS_BBB score ranges from 0 to 6, where a score < 3 indicates low/null brain penetration.
[b] CNS_MPO score ranges from 0 to 6, where a score < 3 indicates low/null brain penetration.

studies targeting GPR17 expressed in brain should take into account these parameters and hypothesize special delivery systems like nanocarriers or nanoparticles. The modification of the compounds by inserting phosphate-masking groups (hence obtaining prodrugs) could be an alternative approach.

It must be underlined that the ADMET prediction tools are not optimized for the analysis of polyphosphate (and in generale polyanionic) compounds, hence the predicted values and pharmacokinetic profile of the newly synthesized nucleotide compounds could present inaccuracies and should require experimental methods for a more reliable analysis.

3. Conclusions

GPR17 plays a key role in neurodegenerative disorders and could be a potential therapeutic target for multiple sclerosis, cerebral ischemia, traumatic brain injury, and spinal cord injury. We report in this study the design and synthesis of new adenine nucleotides, which behave as potent agonists and antagonists of GPR17 in a cAMP assay. **10** Is an agonist having a picomolar activity at the GPR17 receptor (62 pM), whereas **16** shows a low nanomolar antagonist profile (13 nM). Comparative evaluation of a set of these newly synthesized compounds (**1**, **9**, and **10**) at the $G\alpha_{i/o}$ protein-coupled $hP2Y_{12}$, $hP2Y_{13}$, and $hP2Y_{14}$ showed that their interaction with these protein occurs at concentrations much higher than the ones needed to obtain a decrease of cAMP through GPR17 stimulation, demonstrating the selective effect of these three compounds at the GPR17 at low nanomolar (or picomolar) concentrations. Molecular modeling studies were performed to provide an hypothetical binding mode of the compounds at an homology model of the hGPR17. Given the high hydrophilicity of the presented compounds, a very low blood-brain barrier crossing and a very low brain penetration are expected. Hence, an *in vivo* application of these molecules for brain disorders could be possible only with the setup of systems like nanoparticles/nanocarriers allowing a brain-targeted delivery, or by modifying the compounds by masking the phosphate groups to obtain prodrugs. Such systems could be set up also to prevent metabolism occurring to triphosphate and triphosphate-modified derivatives. Still, the triphosphate and triphosphate-modified analogues presented in this work may represent potent instruments to be added to the currently available pharmacological tools, for further characterization of the elusive GPR17 receptor *in vitro* and in various physio-pathological events.

4. Experimental section

4.1. Chemistry

Melting points were determined with a Büchi apparatus B-540. ^{1}H and ^{31}P NMR spectra (202.45 MHz) were obtained with Varian Mercury 400 MHz spectrometer; δ in ppm, J in Hz. All exchangeable protons were confirmed by the addition of D_2O. ^{13}C NMR spectra (for final nucleotides; in the case of **13** the low amount of available compound furnished a not defined ^{13}C NMR spectra, hence, a ^{13}C NMR spectra of the precursor nucleoside **12** is reported) were obtained with Bruker Mercury 500 MHz spectrometer (125.77 MHz). Thin-layer chromatography (TLC) was carried out on pre-coated TLC plates with silica gel 60 F-254 (Merck). For column chromatography, silica gel 60 (Merck) was used. For ion exchange chromatography, a Sephadex® DEAE A-25 resin HCO_3^- form was used. Mass spectra were recorded on an HP 1100-MSD series instrument. All measurements were performed using electrospray ionization (ESI-MS) on a single quadrupole analyzer. Elemental analyses were determined on a Fisons model EA 1108 CHNS–O model analyzer and are within ±0.4% of theoretical values. Purity of the compounds was ≥95% according to elemental analysis data.

4.1.1. 6-Chloro-2-phenylethynyl-9-(2′,3′,5′-tri-O-acetyl-β-D-ribofuranosyl) purine (5)

$(Ph_3P)_2PdCl_2$ (42 mg, 0.0033 mmol), CuI (2.6 mg, 13.65 mmol), triethylamine (10.4 mL, 74.11), and phenylethyne (0.253 mL, 2.23 mmol) were added in a solution of compound **4** (1.0 g, 1.86 mmol) in dry DMF (40 mL) under N_2 atmosphere. Then reaction was left at room temperature for 3 h. Volatiles were removed under vacuo and the crude was chromatographed by silica flash column eluting with $CHCl_3$-cHex (80:20, *v*/v). Impure fractions were purified by silica gel normal column eluting with EtOAc-nHex (1:1, v/v) to obtain **5** as a vitreous solid (0.80 g, 1.56 mmol). Yield 84%; mp 71–73 °C. ^{1}H NMR (DMSO-d_6): δ 2.00 (s, 3H, CH_3), 2.04 (s, 3H, CH_3), 2.12 (s, 3H, CH3), 4.31 (m, 1H, *H*-CH-5′), 4.39 (m, 1H, H-4′), 4.43 (m, 1H, *H*-CH-5′), 5.69 (m, 1H, H-3′), 5.94 (m, 1H, H-2′), 6.36 (d, J = 5.2 Hz, 1H, H-1′), 7.52 (m, 3H, H-Ph), 7.70 (m, 2H, H-Ph), 8.97 ppm (s, 1H, H-8).

4.1.2. 2-Phenylethynyladenosine (6)

Liquid ammonia was condensed at −78 °C into a steel vessel, then **5** (200 mg, 0.38 mmol) was added, and the reaction mixture was maintained at room temperature for 16 h. After removing volatiles, the mixture was chromatographed eluting with DCM-MeOH (90:10, v/v) to obtain pure product **6** as a white solid (110 mg, 0.30 mmol). Yield 78%; mp 215–216 °C. ^{1}H NMR (DMSO-d_6): δ 3.57 (m, 1H, *H*-CH-5′), 3.66 (m, 1H, *H*-CH-5′), 3.95 (q, J = 3.2 Hz, 1H, H-4′), 4.12 (q, J = 3.6 Hz, 1H, H-3′), 4.54 (q, J = 5.6 Hz, 1H, H-2′), 5.22 (m, 2H, 2 x OH), 5.47 (m, 1H, OH), 5.89 (d, J = 6.4 Hz, 1H, H-1′), 7.45 (m, 3H, H-Ph), 7.58 (m, 4H, H-Ph and NH_2), 8.44 ppm (s, 1H, H-8).

4.1.3. N^6-Methyl-2-phenylethynyladenosine (7)

Compound **5** (240 mg, 0.47 mmol) was taken into a steel vial at −20 °C then CH_3NH_2 (1.5 mL) was added. The mixture was left at room temperature for 30 min. Volatiles were removed under vacuo and the final compound **7** was obtained pure after crystallization from CH_3CN as a white solid (118 mg, 0.31 mmol). Yield 66%; mp 152–155 °C. ^{1}H NMR (DMSO-d_6): δ 2.96 (m, 3H, CH_3), 3.57 (m, 1H, *H*-CH-5′), 3.65 (m, 1H, *H*-CH-5′), 3.95 (m, 1H, H-4′), 4.13 (m, 1H, H-3′), 4.54 (q, J = 5.6 Hz, 1H, H-2′), 5.21 (d, J = 4.4 Hz, 1H, OH), 5.25 (t, J = 6.4 Hz, 1H, OH), 5.48 (d, J = 6.4 Hz, 1H, OH), 5.89 (d, J = 6.4 Hz, 1H, H-1′), 7.45 (m, 3H, Ph), 7.61 (m, 2H, Ph), 7.99 (m, 1H, NH), 8.43 ppm (s, 1H, H-8).

4.1.4. N^6-Methyl-2-phenylethynyladenosine-5′-O-triphosphate tetraammonium salt (8)

The lyophilized nucleoside **7** (200 mg, 0.52 mmol) and proton sponge (0.78 mmol) were suspended in trimethyl phosphate (5.2 mL) at 0 °C and phosphorous oxychloride (0.99 mmol) was added. The mixture was left under stirring in N_2 atmosphere at room temperature for 3 h after which the suspension was completely clear. In the meantime, tributylammonium pyrophosphate (3.3 mmol) was solubilized with DMF (5.2 mL) and tributylamine (2.0 mmol) was added. When the mixture became clear, this was added to the previous reaction mixture

and left under stirring at room temperature under N_2 atmosphere for 90 min. To the formed suspension, 12.5 mL of a cooled solution of 0.5 M TEAB (4 °C) was added to quench the reaction and the mixture was left under stirring for 4 min. Then mixture was lyophilized and crude was purified by ionic exchange chromatography on a Sephadex® DEAE A-25 (Fluka) column (HCO_3^- form) equilibrated with H_2O and eluted with a linear gradient of 0 to 0.5 M NH_4HCO_3 aqueous solution. Fractions were collected, and appropriate fractions were selected and concentrated under vacuum and lyophilized several times to remove NH_4HCO_3 yielding the pure nucleotide **8** as a white foam (39 mg, 0.057 mmol). Yield 11%. ^{1}H NMR (D_2O): δ 2.94 (br s, 3H, CH_3), 4.10 (m, 2H, CH_2–5′), 4.25 (m, 1H, H-4′), 4.43 (m, 1H, H-3′), 4.57 (m, 1H, H-2′), 5.91 (d, J = 4.8 Hz, 1H, H-1′), 7.17 (m, 3H, H-Ph), 7.36 (m, 2H, H-Ph), 8.28 ppm (s, 1H, H-8); ^{13}C NMR (D_2O): δ 27.45 (NCH_3), 65.23 (C5'), 70.28 (C3'), 74.58 (C2'), 83.98 (C4'), 86.86 (C1'), 87.34 (C≡), 118.55 (≡C), 120.26 (C5), 128.58 (2xC-Ph), 129.98 (C-Ph), 132.08 (2xC-Ph), 139.68 (C8), 146.58 (C4), 148.19 (C2), 155.41 (C6) ppm; ^{31}P NMR (D_2O): δ 8.58, 10.34, 21.77 ppm. *M/z*: [calculated M.W. = 621.3] Negative mode: 642.0 $[M\text{-}2H\text{+}Na]^-$.

4.1.5. 2-Phenylethynyladenosine-5'-O-(α,β-methylenetriphosphate) tetratriethylammonium salt (9)

A cooled solution of methylenediphosphonic dichloride (0.135 g, 0.54 mmol) in trimethylphosphate (4 mL) was added to a suspension of **6** (100 mg, 0.27 mmol) in trimethylphosphate (4 mL) at 0 °C under N_2 atmosphere. The reaction mixture was left for 4.5 h. Then tributylamine (1.5 mL) and phosphorylating reagent (nBu$_3$N)H$_3$PO$_4$ (385 mg, 1.36 mmol) were added, and the mixture was left stirring for 30 min. It was then quenched with 10 mL of cooled solution of 0.5 M TEAB (4 °C) and stirred for 15 min. The reaction mixture was allowed to warm to room temperature and left for 1 h. Trimethylphosphate was extracted in *tert*-butyl methyl ether (3 × 20 mL) and the mixture was lyophilized. The residue was purified by ionic exchange chromatography on a Sephadex® DEAE A-25 (Fluka) column (HCO_3^- form) equilibrated with H_2O and eluted with a linear gradient of 0.5 M TEAB to 1 M TEAB. Nucleotide **9** was obtained after lyophilization as a white solid (87 mg, 0.086 mmol). Yield 16%. ^{1}H NMR (D_2O): δ 1.14 (m, 27H, NCH_2CH_3), 2.26 (t, J = 20.0 Hz, 2H, CH_2), 2.94 (m, 18H, NCH_2CH_3), 4.08 (m, 2H, CH_2–5′), 4.24 (m, 1H, H-4′), 4.40 (m, 1H, H-3′), 4.58 (m, 1H, H-2′), 5.87 (s, 1H, H-1′), 7.11 (m, 3H, H-Ph), 7.31 (m, 2H, H-Ph), 8.43 ppm (s, 1H, H-8); ^{13}C NMR (D_2O): δ 8.40 (CH_3), 46.79 (CH_2), 63.77 (C5'), 70.27 (C3'), 74.72 (C2'), 84.12 (C4'), 86.01 (C≡), 87.41 (C1'), 88.32 (PCH_2P), 117.90 (≡C), 119.87 (C5), 128.69 (2xC-Ph), 130.26 (C-Ph), 132.31 (2xC-Ph), 140.97 (C8), 144.84 (C4), 149.04 (C2), 154.48 (C6) ppm; ^{31}P NMR (D_2O): δ − 9.78, 7.60, 18.52 ppm.

4.1.6. General procedure for the synthesis of $P_\alpha P_\beta$-dichloromethylene nucleotides 10 and 16

The dry nucleoside, **6** or **15**, (1 mmol) was dissolved in 5 mL of trimethylphosphate and the mixture was stirred at room temperature under N_2 flow and then cooled to 4 °C. Dry proton sponge (1.5 mmol) was added followed by $POCl_3$ (3 mmol) 5 min later. After stirring for 3 h at 0 °C, tributylamine (0.72 mmol) was added to the solution followed by 10 mL (5 mmol) of 0.5 M bis-(tributylammonium) dichloromethylene bisphosphonate solution in DMF. After 5 min, the mixture was poured into a cold 0.5 M aqueous TEAB solution and stirred at 0 °C for several minutes. The stirred solution was left to warm to RT and left standing for 1 h. Trimethylphosphate was extracted with *tert*-butylmethyl ether, and the aqueous was evaporated and freeze-dried to yield glassy oils. These crudes were purified by ion exchange chromatography using Sephadex® DEAE A-25 gel HCO_3^- form. After equilibration of the column with deionized H_2O (2 L), the crude product was dissolved in 2 mL deionized H_2O and poured into the column. The column was washed with deionized water (500 mL), followed by a solvent gradient of 0 to 0.5 M NH_4HCO_3 buffer (800 mL) for **10** or TEAB buffer (800 mL) for **16**. Fractions were collected, and appropriate fractions were selected and concentrated under vacuum and lyophilized several times to remove NH_4HCO_3. The residue was further purified over the Sephadex® column using the same previously described procedure. Fractions were collected, and appropriate fractions were concentrated under vacuum and freeze-dried several times to remove NH_4HCO_3, yielding the pure nucleotides.

4.1.6.1. 2-Phenylethynyladenosine-5'-O-(β,γ-dichloromethylenetriphosphate) tetraammonium salt (10).

Nucleoside **6** (200 mg, 0.54 mmol) was used for the synthesis yielding **10** (28.0 mg, 0.038 mmol) in 7% yield. ^{1}H NMR (D_2O): δ 4.12 (m, 2H, CH_2–5′), 4.25 (m, 1H, H-4′), 4.43 (m, 1H, H-3′), 4.59 (m, 1H, H-2′), 5.96 (m, 1H, H-1′), 7.28 (m, 3H, H-Ph), 7.49 (m, 2H, H-Ph), 8.40 ppm (s, 1H, H-8); ^{13}C NMR (D_2O): δ 65.32 (C5'), 70.17 (C3'), 74.82 (C2'), 83.69 (C4'), 86.89 (C1'), 87.08 (C≡), 87.41 (CCl_2), 118.47 (≡C), 120.06 (C5), 128.36 (2C-Ph), 129.93 (C-Ph), 132.15 (2C-Ph), 140.15 (C8), 146.16 (C4), 155.38 (C2), 157.73 (C6) ppm; ^{31}P NMR (D_2O): δ − 9.70, 1.35, 8.30 ppm.

4.1.6.2. N^6-methyladenosine-5'-O-(β,γ-dichloromethylenetriphosphate) triethylammonium salt (16).

Nucleoside **15** (200 mg, 0.72 mmol) was used for the synthesis yielding **16** (38.0 mg, 0.058 mmol) in 8% yield. ^{1}H NMR (D_2O): δ 1.18 (m, 27H, NCH_2CH_3), 2.93 (s, 3H, CH_3), 3.21 (m, 18H, NCH_2CH_3), 4.08 (m, 1H, *H*-CH-5′), 4.15 (m, 1H, *H*-CH-5′), 4.23 (m, 1H, H-4′), 4.46 (m, 1H, H-3′), 4.61 (m, 1H, H-2′), 5.96 (d, J = 6.0 Hz, 1H, H-1′), 8.10 (s, 1H, H-2), 8.32 ppm (s, 1H, H-8); ^{13}C NMR (D_2O): δ 8.24 (CH_3), 27.65 (NCH_3), 46.83 (CH_2), 65.55 (C5'), 70.48 (C3'), 74.52 (C2'), 84.06 (CCl_2), 84.11 (C4'), 86.95 (C1'), 119.02 (C5), 139.38 (C8), 147.54 (C4), 153.17 (C2), 155.41 (C6) ppm; ^{31}P NMR (D_2O): δ − 9.82, 1.93, 8.71 ppm.

4.1.7. 2-Phenylethynyl-2′-deoxyadenosine (12)

$(Ph_3P)_2PdCl_2$ (6.4 mg, 0.009), CuI (40 mg), triethylamine (1.7 mL), and phenylethyne (0.526 mL, 4.8 mmol) were added in a solution of **11** (150 mg, 0.40 mmol) in dry DMF (40 mL) and under N_2 atmosphere. The reaction was left at room temperature for 7 h. Volatiles were removed under vacuo and the crude was chromatographed by silica flash column eluting with $CHCl_3$-CH_3OH (90:10, *v*/v). Impure fractions were purified by silica gel normal column eluting with $CHCl_3$-*c*Hex-CH_3OH (63:25:12 v/v/v) to obtain **12** as a white solid (109.7 mg, 0.39 mmol). Yield 97%. ^{1}H NMR (DMSO-d_6): δ 2.30 (m, 1H, *H*-CH-2′), 2.64 (m, 1H, *H*-CH-2′), 3.58 (m, 2H, CH_2–5′), 3.88 (m, 1H, H-4′), 4.39 (m, 1H, H-3′), 5.09 (t, J = 5.06 Hz, 1H, OH-5′), 5.11 (d, J = 5.09 Hz, 1H, OH-3′), 6.35 (t, J = 6.38 Hz, 1H, H-1′), 7.40 (m, 7H, phenyl and NH_2), 8.44 ppm (1H, s, H-8). ^{13}C NMR (D_2O): δ 62.24 (C5'), 71.27 (C3'), 83.60 (C2'), 84.02 (C4'), 88.48 (C1'), 89.92 (C≡), 119.21 (≡C), 121.73 (C5), 129.35 (2xC-Ph), 129.97 (C-Ph), 132.32 (2xC-Ph), 140.65 (C8), 145.82 (C4), 149.58 (C2), 156.38 (C6) ppm.

4.1.8. 2-Phenylethynyl-2′-deoxyadenosine-3′,5′-bisphosphate bisammonium salt (13)

Dry proton sponge (64 mg, 0.30 mmol) was added at room temperature to a stirred suspension of **12** (53 mg, 0.15 mmol) and trimethyl phosphate (75 μL) under nitrogen atmosphere. The reaction mixture was cooled at 0 °C, then $POCl_3$ (56 μL, 0.60 mmol) was added and the reaction was left at room temperature for 1 h. The mixture was cooled at 0 °C, 1.5 mL of water was added and then it was neutralized with triethylamine. When the suspension became clear, it was lyophilized and the crude was purified by means of ionic exchange chromatography on a Sephadex® DEAE A-25 (Fluka) column (HCO_3^- form) equilibrated with H_2O and eluted with a linear gradient of 0.5 M to 1 M NH_4HCO_3. After lyophilization of the appropriate fractions, pure product **13** was obtained as a white powder (15 mg, 0.027 mmol). Yield 18%. ^{1}H NMR (D_2O): δ 2.61 (m, 2H, H-2′), 3.77 (m, 2H, CH_2–5′), 4.27 (s, 1H, H-3′), 6.34 (m, 1H, H-1′), 7.29 (m, 3H, H-Ph), 7.51 (d, J = 7.2 Hz, 2H, H-Ph), 8.49 ppm (s, 1H, H-8). ^{31}P NMR (D_2O): δ 4.92; 4.36 ppm; Mass: 254.6 [M-

2H]$^{2-}$/2.

4.1.9. 6-Iodo-9-(β-D-ribofuranosyl)purine (14)

Isoamyl nitrite (10.6 mL, 78.90 mmol) was added to a stirred solution of adenosine (1.0 g, 3.74 mmol) and diiodomethane (7.5 mL, 93.5 mmol) in DMF (12 mL), and the mixture was heated at 60 °C for 30 min. After removal of volatiles, the residue was made into a slurry and purified by flash chromatography, eluting with $CHCl_3$/MeOH (95:5, *v*/v), to afford **14** as a white solid after recrystallization from EtOAc (302 mg, 0.60 mmol). Yield 16%; mp 156–158 °C. ^{1}H NMR (DMSO-d_6): δ 3.62 (m, 2H, CH_2–5′), 3.97 (m, 1H, H-4′), 4.17 (m, 1H, H-3′), 4.57 (m, 1H, H-2′), 5.10 (m, 1H, OH), 5.25 (m, 1H, OH), 5.57 (m, 1H, OH), 5.99 (d, J = 5.2 Hz, 1H, H-1′), 8.65 (s, 1H, H-2), 8.90 ppm (s, 1H, H-8).

4.1.10. N^6-methyladenosine (15)

Methylamine (2 mL) was added to compound **14** (200 mg, 0.40 mmol) in a steel vessel at −80 °C. The steel vessel was sealed and left at room temperature for 3 h, after which the excess methylamine was left to escape under the hood. The residue was collected and purified over a flash column eluting with $CHCl_3$/MeOH (90:10, v/v) to obtain the desired product **15** (78 mg, 0.28 mmol). Yield 69%; mp 130–132 °C. ^{1}H NMR (DMSO-d_6): δ 2.95 (br s, 3H, CH_3), 3.60 (m, 2H, CH_2–5′), 3.95 (m, 1H, H-4′), 4.13 (m, 1H, H-3′), 4.60 (m, 1H, H-2′), 5.17 (m, 1H, OH), 5.41 (m, 2H, 2 x OH), 5.87 (d, J = 6.2 Hz, 1H, H-1′), 7.80 (s, 1H, NH), 8.21 (s, 1H, H-2), 8.33 ppm (s, 1H, H-8).

4.2. Biological evaluation

The pharmacological assay was performed following a previously reported procedure [32].

4.2.1. Cell culture

HEK293 L9–2 cells, kindly provided by Promega Corporation (Madison, WI, USA), were maintained under adherent culture conditions in high-glucose Dulbecco's Modified Eagle Medium (DMEM). The medium was supplemented with 10% foetal bovine serum (FBS), 20 mM L-glutamine, 1% sodium pyruvate, 1% penicillin–streptomycin, 1% amphotericin B, and 0.2 mg/mL hygromycin. Cells were cultured at 37 °C in a humidified incubator with 5% CO_2 and 95% O_2.

4.2.2. Transient transfection

Cells were plated in six-well culture plates and transfected upon reaching approximately 80% confluence using the Arrest-In transfection reagent. Briefly, 3 μg of *hgpr*17 (or *hp*2*y*12, or *hp*2*y*13, or *hp*2*y*14) plasmid DNA and 15 μL of Arrest-In reagent were each separately diluted in serum-free medium. The diluted DNA was then combined with the diluted Arrest-In reagent, gently mixed, and allowed to complex for 20 min at room temperature in accordance with the manufacturer's instructions. The resulting DNA–Arrest-In complexes were added to the cells, which were subsequently incubated for 6 h at 37 °C in a CO_2-controlled incubator. Following this incubation period, the transfection mixture was removed and replaced with fresh complete medium supplemented with 10% FBS. Cells were maintained for an additional 48 h before being used for the GloSensor cAMP assay.

4.2.3. GloSensor cAMP assay

Cells were harvested in CO_2-independent medium and counted using a Neubauer chamber. The appropriate number of cells was resuspended in an equilibration medium consisting of CO_2-independent medium supplemented with 10% FBS, 3% (*v*/v) GloSensor cAMP reagent stock solution and 87% CO_2 independent medium. Following a 2 h equilibration period, cells were dispensed into 384-well plates. Once a stable basal luminescent signal was achieved, agonists were added at increasing concentrations.

The antagonist activity of the tested compounds was determined by measuring their ability to inhibit the agonist-induced reduction of intracellular cAMP levels. Cells were preincubated with varying concentrations of antagonists in reaction medium for 10 min at room temperature, after which agonists were added. Forskolin (FSK, 10 μM) was subsequently added 10 min after agonist stimulation, and luminescence signals were measured at various time intervals.

None of the compounds tested produced measurable changes in basal luminescence or in the cAMP response elicited by forskolin.

4.2.4. Statistical analysis

Responses were expressed as a percentage of the maximal relative luminescence units (RLU), with the response elicited by UDP defined as 100%. Concentration–response curves were generated by nonlinear regression analysis using Prism 5.0 software (GraphPad Software, San Diego, CA, USA). Agonist potency was quantified by calculating half-maximal effective concentration (EC_{50}) values. Antagonist activity was assessed by determining half-maximal inhibitory concentration (IC_{50}) values, defined as the antagonist concentration required to inhibit 50% of the agonist-induced response. Each concentration was evaluated in triplicate across five independent experiments, and data are presented as mean ± standard error (SE).

4.2.5. Molecular modeling studies

An homology model of the hGPR17 was developed by using the X-Ray structure of the $hP2Y_{12}$ receptor complexed with the agonist 2-methylthio-ADP (pdb code: 4PXZ [40]) as a template. The homology modeling study, together with receptor model refinement with energy minimization tools, was performed within Molecular Operating Environment (MOE2022.02) Suite [41].

All compound were docked into the hGPR17 binding site using the Induced Fit docking protocol of MOE [41] and the genetic algorithm docking tool of CCDC Gold [42]. The Induced Fit docking protocol of MOE consists in a conformational analysis of compounds followed by rigid docking of the generated conformations into the binding site of the target. All the poses are then scored by the MOE *Alpha HB* scoring function. Top 50 poses were energetically minimized within the binding site, together with the side chains of aminoacids of the cavity. All the generated complexes are then subjected to re-scoring with the *Alpha HB* scoring function. Gold docking analysis was set up with default efficiency settings, by selecting Chemscore, ASP, and PLP as scoring functions. All docking conformations were energetically minimized within MOE interface, by leaving unconstrained the whole receptor structure. Once energetically minimized, the top scored conformations for each compound were selected for visualization and analysis, with focus on the most populated families of top score conformations.

CRediT authorship contribution statement

Diego Dal Ben: Writing – review & editing, Writing – original draft. **Catia Lambertucci:** Writing – review & editing, Writing – original draft, Methodology, Investigation, Data curation. **Michela Buccioni:** Writing – review & editing, Writing – original draft, Methodology, Investigation, Data curation. **Beatrice Francucci:** Data curation. **Andrea Spinaci:** Data curation. **Rosaria Volpini:** Writing – review & editing, Supervision, Investigation, Conceptualization. **Gabriella Marucci:** Writing – review & editing, Investigation, Conceptualization.

Declaration of competing interest

The authors declare that they have no known competing financial interests or personal relationships that could have appeared to influence the work reported in this paper.

Acknowledgement

This research was funded by Fondo di Ateneo-per la Ricerca Scientifica (University of Camerino).

Appendix A. Supplementary data

Supplementary data to this article can be found online at https://doi.org/10.1016/j.bioorg.2026.109567.

Data availability

No data was used for the research described in the article.

References

[1] P. Ciana, M. Fumagalli, M.L. Trincavelli, C. Verderio, P. Rosa, D. Lecca, S. Ferrario, C. Parravicini, V. Capra, P. Gelosa, U. Guerrini, S. Belcredito, M. Cimino, L. Sironi, E. Tremoli, G.E. Rovati, C. Martini, M.P. Abbracchio, The orphan receptor GPR17 identified as a new dual uracil nucleotides/cysteinyl-leukotrienes receptor, EMBO J. 25 (2006) 4615–4627, https://doi.org/10.1038/sj.emboj.7601341.

[2] D. Lecca, M.L. Trincavelli, P. Gelosa, L. Sironi, P. Ciana, M. Fumagalli, G. Villa, C. Verderio, C. Grumelli, U. Guerrini, E. Tremoli, P. Rosa, S. Cuboni, C. Martini, A. Buffo, M. Cimino, M.P. Abbracchio, The recently identified P2Y-like receptor GPR17 is a sensor of brain damage and a new target for brain repair, PLoS One 3 (2008) e3579, https://doi.org/10.1371/journal.pone.0003579.

[3] G. Marucci, D. Dal Ben, C. Lambertucci, C. Santinelli, A. Spinaci, A. Thomas, R. Volpini, M. Buccioni, The G protein-coupled receptor GPR17: overview and update, ChemMedChem 11 (2016) 2567–2574, https://doi.org/10.1002/cmdc.201600453.

[4] A. Keifi Bajestani, M.S. Alavi, L. Etemad, A. Roohbakhsh, Role of orphan G-protein coupled receptors in tissue ischemia: a comprehensive review, Eur. J. Pharmacol. 978 (2024) 176762, https://doi.org/10.1016/j.ejphar.2024.176762.

[5] Y. Chen, H. Wu, S. Wang, H. Koito, J. Li, F. Ye, J. Hoang, S.S. Escobar, A. Gow, H. A. Arnett, B.D. Trapp, N.J. Karandikar, J. Hsieh, Q.R. Lu, The oligodendrocyte-specific G protein-coupled receptor GPR17 is a cell-intrinsic timer of myelination, Nat. Neurosci. 12 (2009) 1398–1406, https://doi.org/10.1038/nn.2410.

[6] M. Fumagalli, S. Daniele, D. Lecca, P.R. Lee, C. Parravicini, R.D. Fields, P. Rosa, F. Antonucci, C. Verderio, M.L. Trincavelli, P. Bramanti, C. Martini, M. P. Abbracchio, Phenotypic changes, signaling pathway, and functional correlates of GPR17-expressing neural precursor cells during oligodendrocyte differentiation, J. Biol. Chem. 286 (2011) 10593–10604, https://doi.org/10.1074/jbc.M110.162867.

[7] S. Ceruti, F. Vigano, E. Boda, S. Ferrario, G. Magni, M. Boccazzi, P. Rosa, A. Buffo, M.P. Abbracchio, Expression of the new P2Y-like receptor GPR17 during oligodendrocyte precursor cell maturation regulates sensitivity to ATP-induced death, Glia 59 (2011) 363–378, https://doi.org/10.1002/glia.21107.

[8] E. Boda, F. Vigano, P. Rosa, M. Fumagalli, V. Labat-Gest, F. Tempia, M. P. Abbracchio, L. Dimou, A. Buffo, The GPR17 receptor in NG2 expressing cells: focus on in vivo cell maturation and participation in acute trauma and chronic damage, Glia 59 (2011) 1958–1973, https://doi.org/10.1002/glia.21237.

[9] H. Franke, C. Parravicini, D. Lecca, E.R. Zanier, C. Heine, K. Bremicker, M. Fumagalli, P. Rosa, L. Longhi, N. Stocchetti, M.G. De Simoni, M. Weber, M. P. Abbracchio, Changes of the GPR17 receptor, a new target for neurorepair, in neurons and glial cells in patients with traumatic brain injury, Purinergic Signal 9 (2013) 451–462, https://doi.org/10.1007/s11302-013-9366-3.

[10] S. Ceruti, G. Villa, T. Genovese, E. Mazzon, R. Longhi, P. Rosa, P. Bramanti, S. Cuzzocrea, M.P. Abbracchio, The P2Y-like receptor GPR17 as a sensor of damage and a new potential target in spinal cord injury, Brain 132 (2009) 2206–2218, https://doi.org/10.1093/brain/awp147.

[11] S. Hennen, H. Wang, L. Peters, N. Merten, K. Simon, A. Spinrath, S. Blattermann, R. Akkari, R. Schrage, R. Schroder, D. Schulz, C. Vermeiren, K. Zimmermann, S. Kehraus, C. Drewke, A. Pfeifer, G.M. Konig, K. Mohr, M. Gillard, C.E. Müller, Q. R. Lu, J. Gomeza, E. Kostenis, Decoding signaling and function of the orphan G protein-coupled receptor GPR17 with a small-molecule agonist, Sci. Signal. 6 (2013) ra93, https://doi.org/10.1126/scisignal.2004350.

[12] C.J. Raport, V.L. Schweickart, D. Chantry, R.L. Eddy Jr., T.B. Shows, R. Godiska, P. W. Gray, New members of the chemokine receptor gene family, J. Leukoc. Biol. 59 (1996) 18–23, https://doi.org/10.1002/jlb.59.1.18.

[13] D. Basrai, R. Kraft, C. Bollensdorff, L. Liebmann, K. Benndorf, S. Patt, BK channel blockers inhibit potassium-induced proliferation of human astrocytoma cells, Neuroreport 13 (2002) 403–407, https://doi.org/10.1097/00001756-200203250-00008.

[14] A.M. Pugliese, M.L. Trincavelli, D. Lecca, E. Coppi, M. Fumagalli, S. Ferrario, P. Failli, S. Daniele, C. Martini, F. Pedata, M.P. Abbracchio, Functional characterization of two isoforms of the P2Y-like receptor GPR17: [^{35}S]GTPgammaS binding and electrophysiological studies in 1321N1 cells, Am. J. Phys. Cell Phys. 297 (2009) C1028–C1040, https://doi.org/10.1152/ajpcell.00658.2008.

[15] T. Benned-Jensen, M.M. Rosenkilde, Distinct expression and ligand-binding profiles of two constitutively active GPR17 splice variants, Br. J. Pharmacol. 159 (2010) 1092–1105, https://doi.org/10.1111/j.1476-5381.2009.00633.x.

[16] K. Simon, S. Hennen, N. Merten, S. Blattermann, M. Gillard, E. Kostenis, J. Gomeza, The orphan G protein-coupled receptor GPR17 negatively regulates oligodendrocyte differentiation via Galphai/o and its downstream effector molecules, J. Biol. Chem. 291 (2016) 705–718, https://doi.org/10.1074/jbc.M115.683953.

[17] D. Lecca, S. Raffaele, M.P. Abbracchio, M. Fumagalli, Regulation and signaling of the GPR17 receptor in oligodendroglial cells, Glia 68 (2020) 1957–1967, https://doi.org/10.1002/glia.23807.

[18] M. Lewash, E. Kostenis, C.E. Müller, GPR17 - orphan G protein-coupled receptor with therapeutic potential, Trends Pharmacol. Sci. 46 (2025) 610–628, https://doi.org/10.1016/j.tips.2025.05.001.

[19] E. Calleri, S. Ceruti, G. Cristalli, C. Martini, C. Temporini, C. Parravicini, R. Volpini, S. Daniele, G. Caccialanza, D. Lecca, C. Lambertucci, M.L. Trincavelli, G. Marucci, I.W. Wainer, G. Ranghino, P. Fantucci, M.P. Abbracchio, G. Massolini, Frontal affinity chromatography-mass spectrometry useful for characterization of new ligands for GPR17 receptor, J. Med. Chem. 53 (2010) 3489–3501, https://doi.org/10.1021/jm901691y.

[20] A. Maekawa, B. Balestrieri, K.F. Austen, Y. Kanaoka, GPR17 is a negative regulator of the cysteinyl leukotriene 1 receptor response to leukotriene D4, Proc. Natl. Acad. Sci. USA 106 (2009) 11685–11690, https://doi.org/10.1073/pnas.0905364106.

[21] A.D. Qi, T.K. Harden, R.A. Nicholas, Is GPR17 a P2Y/leukotriene receptor? Examination of uracil nucleotides, nucleotide sugars, and cysteinyl leukotrienes as agonists of GPR17, J. Pharmacol. Exp. Ther. 347 (2013) 38–46, https://doi.org/10.1124/jpet.113.207647.

[22] C.E. Heise, B.F. O'Dowd, D.J. Figueroa, N. Sawyer, T. Nguyen, D.S. Im, R. Stocco, J. N. Bellefeuille, M. Abramovitz, R. Cheng, D.L. Williams Jr., Z. Zeng, Q. Liu, L. Ma, M.K. Clements, N. Coulombe, Y. Liu, C.P. Austin, S.R. George, G.P. O'Neill, K. M. Metters, K.R. Lynch, J.F. Evans, Characterization of the human cysteinyl leukotriene 2 receptor, J. Biol. Chem. 275 (2000) 30531–30536, https://doi.org/10.1074/jbc.M003490200.

[23] E. Kostenis, A. Spinrath, S. Hennen, L. Peters, C.E. Müller, R. Akkari, Y. Baqi, K. Ritter, Methods of Identifying Modulators of gpr17, US8404436B1, 2013.

[24] Y. Baqi, S. Alshaibani, K. Ritter, A. Abdelrahman, A. Spinrath, E. Kostenis, C. E. Müller, Improved synthesis of 4−/6-substituted 2-carboxy-1*H*-indole-3-propionic acid derivatives and structure–activity relationships as GPR17 agonists, MedChemComm 5 (2014) 86–92, https://doi.org/10.1039/C3MD00309D.

[25] T. Pillaiyar, M. Funke, H. Al-Hroub, S. Weyler, S. Ivanova, J. Schlegel, A. Abdelrahman, C.E. Müller, Design, synthesis and biological evaluation of suramin-derived dual antagonists of the proinflammatory G protein-coupled receptors $P2Y_2$ and GPR17, Eur. J. Med. Chem. 186 (2020) 111789, https://doi.org/10.1016/j.ejmech.2019.111789.

[26] C. Parravicini, D. Lecca, D. Marangon, G.T. Coppolino, S. Daniele, E. Bonfanti, M. Fumagalli, L. Raveglia, C. Martini, E. Gianazza, M.L. Trincavelli, M. P. Abbracchio, I. Eberini, Development of the first in vivo GPR17 ligand through an iterative drug discovery pipeline: a novel disease-modifying strategy for multiple sclerosis, PLoS One 15 (2020) e0231483, https://doi.org/10.1371/journal.pone.0231483.

[27] P. Nguyen, P. Doan, T. Rimpilainen, S. Konda Mani, A. Murugesan, O. Yli-Harja, N. R. Candeias, M. Kandhavelu, Synthesis and preclinical validation of novel indole derivatives as a GPR17 agonist for glioblastoma treatment, J. Med. Chem. 64 (2021) 10908–10918, https://doi.org/10.1021/acs.jmedchem.1c00277.

[28] A.W. Harrington, C. Liu, N. Phillips, D. Nepomuceno, C. Kuei, J. Chang, W. Chen, S. W. Sutton, D. O'Malley, L. Pham, X. Yao, S. Sun, P. Bonaventure, Identification and characterization of select oxysterols as ligands for GPR17, Br. J. Pharmacol. 180 (2023) 401–421, https://doi.org/10.1111/bph.15969.

[29] N.M. Boshta, M. Lewash, M. Kose, V. Namasivayam, S. Sarkar, J.H. Voss, A. J. Liedtke, A. Junker, M. Tian, A. Stossel, M. Rashed, A. Mahal, N. Merten, C. Pegurier, J. Hockemeyer, E. Kostenis, C.E. Müller, Discovery of Anthranilic acid derivatives as antagonists of the pro-inflammatory orphan G protein-coupled receptor GPR17, J. Med. Chem. (2024) 19365–19394, https://doi.org/10.1021/acs.jmedchem.4c01755.

[30] F. Ye, T.S. Wong, G. Chen, Z. Zhang, B. Zhang, S. Gan, W. Gao, J. Li, Z. Wu, X. Pan, Y. Du, Cryo-EM structure of G-protein-coupled receptor GPR17 in complex with inhibitory G protein, MedComm 3 (2022) e159, https://doi.org/10.1002/mco2.159.

[31] G. Marucci, D. Dal Ben, C. Lambertucci, A. Marti Navia, A. Spinaci, R. Volpini, M. Buccioni, GPR17 receptor modulators and their therapeutic implications: review of recent patents, Expert Opin. Ther. Pat. 29 (2019) 85–95, https://doi.org/10.1080/13543776.2019.1568990.

[32] M. Buccioni, G. Marucci, D. Dal Ben, D. Giacobbe, C. Lambertucci, L. Soverchia, A. Thomas, R. Volpini, G. Cristalli, Innovative functional cAMP assay for studying G protein-coupled receptors: application to the pharmacological characterization of GPR17, Purinergic Signal 7 (2011) 463–468, https://doi.org/10.1007/s11302-011-9245-8.

[33] S. Eliahu, A. Martin-Gil, M.J. Perez de Lara, J. Pintor, J. Camden, G.A. Weisman, J. Lecka, J. Sevigny, B. Fischer, 2-MeS-beta,gamma-CCl_2-ATP is a potent agent for reducing intraocular pressure, J. Med. Chem. 53 (2010) 3305–3319, https://doi.org/10.1021/jm100030u.

[34] V. Nair, S.G. Richardson, Modification of nucleic acid bases via radical intermediates: synthesis of Dihalogenated purine nucleosides, Synthesis 1982 (1982) 670–672, https://doi.org/10.1055/s-1982-29896.

[35] A. El-Tayeb, A. Qi, R.A. Nicholas, C.E. Müller, Structural modifications of UMP, UDP, and UTP leading to subtype-selective agonists for $P2Y_2$, $P2Y_4$, and $P2Y_6$ receptors, J. Med. Chem. 54 (2011) 2878–2890, https://doi.org/10.1021/jm1016297.

[36] V. Nair, D.F. Purdy, Synthetic approaches to new doubly modified nucleosides: congeners of cordycepin and related 2′-deoxyadenosine, Tetrahedron 47 (1991) 365–382, https://doi.org/10.1016/S0040-4020(01)90496-X.

[37] F. Fan, B.F. Binkowski, B.L. Butler, P.F. Stecha, M.K. Lewis, K.V. Wood, Novel genetically encoded biosensors using firefly luciferase, ACS Chem. Biol. 3 (2008) 346–351, https://doi.org/10.1021/cb8000414.

[38] B. Binkowski, F. Fan, K. Wood, Engineered luciferases for molecular sensing in living cells, Curr. Opin. Biotechnol. 20 (2009) 14–18, https://doi.org/10.1016/j.copbio.2009.02.013.
[39] H. Ko, I. Fricks, A.A. Ivanov, T.K. Harden, K.A. Jacobson, Structure-activity relationship of uridine 5′-diphosphoglucose analogues as agonists of the human $P2Y_{14}$ receptor, J. Med. Chem. 50 (2007) 2030–2039, https://doi.org/10.1021/jm061222w.
[40] J. Zhang, K. Zhang, Z.G. Gao, S. Paoletta, D. Zhang, G.W. Han, T. Li, L. Ma, W. Zhang, C.E. Muller, H. Yang, H. Jiang, V. Cherezov, V. Katritch, K.A. Jacobson, R.C. Stevens, B. Wu, Q. Zhao, Agonist-bound structure of the human $P2Y_{12}$ receptor, Nature 509 (7498) (2014) 119–122, https://doi.org/10.1038/nature13288.
[41] Molecular Operating Environment, C.C.G., Inc, 1255 University St., Suite 1600, Montreal, Quebec, Canada, H3B 3X3, 2026.
[42] G. Jones, P. Willett, R.C. Glen, A.R. Leach, R. Taylor, Development and validation of a genetic algorithm for flexible docking, J. Mol. Biol. 267 (3) (1997) 727–748, https://doi.org/10.1006/jmbi.1996.0897.
[43] M. Gupta, H.J. Lee, C.J. Barden, D.F. Weaver, The blood-brain barrier (BBB) score, J. Med. Chem. 62 (2019) 9824–9836, https://doi.org/10.1021/acs.jmedchem.9b01220.
[44] T.T. Wager, X. Hou, P.R. Verhoest, A. Villalobos, Moving beyond rules: the development of a central nervous system multiparameter optimization (CNS MPO) approach to enable alignment of druglike properties, ACS Chem. Neurosci. 1 (2010) 435–449, https://doi.org/10.1021/cn100008c.